



Dresselhaus effect in bulk wurtzite materials

Wan-Tsang Wang, C. L. Wu, S. F. Tsay, M. H. Gau, Ikai Lo, H. F. Kao, D. J. Jang, Jih-Chen Chiang, Meng-En Lee, Yia-Chung Chang, Chun-Nan Chen, and H. C. Hsueh

Citation: [Applied Physics Letters](#) **91**, 082110 (2007); doi: 10.1063/1.2775038

View online: <http://dx.doi.org/10.1063/1.2775038>

View Table of Contents: <http://scitation.aip.org/content/aip/journal/apl/91/8?ver=pdfcov>

Published by the [AIP Publishing](#)

Articles you may be interested in

[Tensile strained Ge tunnel field-effect transistors: k-p material modeling and numerical device simulation](#)
J. Appl. Phys. **115**, 044505 (2014); 10.1063/1.4862806

[An atomistic-based correction of the effective-mass approach for investigating quantum dots](#)
J. Appl. Phys. **104**, 104309 (2008); 10.1063/1.3021059

[Physics of strain effects in semiconductors and metal-oxide-semiconductor field-effect transistors](#)
J. Appl. Phys. **101**, 104503 (2007); 10.1063/1.2730561

[Effects of lattice mismatch and bulk anisotropy on interband tunneling in broken-gap heterostructures](#)
J. Appl. Phys. **97**, 063704 (2005); 10.1063/1.1857058

[Dependence of optical gain on crystal orientation in wurtzite–GaN strained quantum-well lasers](#)
J. Appl. Phys. **82**, 1518 (1997); 10.1063/1.365951

AIP | Chaos

CALL FOR APPLICANTS

Seeking new Editor-in-Chief

Dresselhaus effect in bulk wurtzite materials

Wan-Tsang Wang, C. L. Wu, S. F. Tsay, M. H. Gau, Ikai Lo, H. F. Kao,
D. J. Jang, and Jih-Chen Chiang^{a)}

*Department of Physics, Center for Nanoscience and Nanotechnology, National Sun Yat-Sen University,
Kaohsiung 80424, Taiwan*

Meng-En Lee^{b)}

*Department of Physics, National Kaohsiung Normal University, Yanchao Township, Kaohsiung County
80424, Taiwan*

Yia-Chung Chang

Research Center for Applied Sciences, Academia Sinica, Taipei 11529, Taiwan

Chun-Nan Chen and H. C. Hsueh

Department of Physics, Tamkang University, Tamsui, Taipei County 25137, Taiwan

(Received 11 July 2007; accepted 31 July 2007; published online 24 August 2007)

The spin-splitting energies of the conduction band for ideal wurtzite materials are calculated within the nearest-neighbor tight-binding method. It is found that ideal wurtzite bulk inversion asymmetry yields not only a spin-degenerate line (along the k_z axis) but also a minimum-spin-splitting surface, which can be regarded as a spin-degenerate surface in the form of $bk_z^2 - k_{\parallel}^2 = 0$ ($b \approx 4$) near the Γ point. This phenomenon is referred to as the Dresselhaus effect (defined as the cubic-in- k term) in bulk wurtzite materials because it generates a term $\gamma_{wz}(bk_z^2 - k_{\parallel}^2)(\sigma_x k_y - \sigma_y k_x)$ in the two-band $\mathbf{k} \cdot \mathbf{p}$ Hamiltonian. © 2007 American Institute of Physics. [DOI: 10.1063/1.2775038]

In recent years a great deal of research in semiconductor physics has been focused on an emerging field—spintronics. One of the most promising proposals is the spin transistor due to Datta and Das.¹ Recently, a different type of spin transistor, the resonant spin lifetime (RSL) transistor is proposed,^{2,3} which is based on the special properties of the spin lifetime tensor due to the interplay between bulk inversion asymmetry (BIA) and structure inversion asymmetry (SIA) in the zinc-blende⁴ or wurtzite⁵ quantum wells (QWs). In the zinc-blende semiconductors, BIA yields a cubic- k term (called Dresselhaus effect)⁶ and SIA leads to a linear- k term (named Rashba effect)⁷ in the two-band $\mathbf{k} \cdot \mathbf{p}$ Hamiltonian. The Dresselhaus and Rashba effects in zinc-blende semiconductors have been well understood because they have been studied intensively by many theoretical methods such as the two-band $\mathbf{k} \cdot \mathbf{p}$, eight-band $\mathbf{k} \cdot \mathbf{p}$, and tight-binding [also known as the linear-combination-of-atomic-orbital (LCAO)] methods.^{6–11} In bulk wurtzite semiconductors, there are two wurtzite bulk inversion asymmetry (WBIA) effects; one is the Dresselhaus effect which leads to a k^3 term in the two-band $\mathbf{k} \cdot \mathbf{p}$ model and the other is the wurtzite structure inversion asymmetry (WSIA) effect, which yields a linear- k term in the two-band $\mathbf{k} \cdot \mathbf{p}$ model.^{12,13} The WSIA effect, which may also be called as the Rashba effect in bulk wurtzite, has been vigorously investigated since 1950s.¹³ However, the Dresselhaus effect in bulk wurtzite is still unknown. In this letter, we shall investigate the Dresselhaus effect in bulk wurtzite within the nearest-neighbor LCAO method.^{10,14} In the nearest-neighbor LCAO model, ideal wurtzite structure ($c/a=0.633$ and $u=d_{\parallel}/c=0.375$, where d_{\parallel} is the length of the bonds parallel to the c axis) yields only the Dresselhaus effect, while deviations from ideal structure generate the WSIA effect.¹² Recently, Tsubaki *et al.*¹⁵ and Lo *et al.*^{16,17}

independently observed a large spin-splitting energy in the two-dimensional electron gases (2DEGs) of GaN/AlGaIn wurtzite heterostructures; moreover, the spin-splitting energy at Fermi surface can be changed dramatically from 0 to 10 meV, by varying the carrier concentrations or the gate voltages.^{15,16} These imply that not only large spin splitting energies¹² but also a spin-degenerate surface¹⁶ exists in the bulk wurtzite semiconductors. In this letter, we shall demonstrate that a cone-shaped minimum-spin-splitting (MSS) surface does exist in the ideal wurtzite Brillouin zone, due to the Dresselhaus effect. Near the Γ point, the MSS surface can be regarded as a spin-degenerate surface because its splitting energies are generally small. Such spin-degenerate surface can be described by an equation of $bk_z^2 - k_{\parallel}^2 = 0$ ($b \approx 4$), where $\mathbf{k}_{\parallel} = k_{\parallel}(\hat{x} \cos \theta + \hat{y} \sin \theta)$, $\mathbf{k}_{x\parallel} \parallel \Gamma\mathbf{M}$, and $\mathbf{k}_{y\parallel} \parallel \Gamma\mathbf{K}$.

To study the Dresselhaus effect in bulk wurtzite, the band structures for ideal wurtzite materials AlN, ZnO, CdS, CdSe, and ZnS are calculated using the nearest-neighbor LCAO method. The LCAO Hamiltonian $H(\mathbf{k})$ can be written in the following form:

$$H(\mathbf{k}) = H_0(\mathbf{k}) + H_{SO}(\mathbf{k}) = \begin{bmatrix} H_0^{\uparrow\uparrow}(\mathbf{k}) & 0 \\ 0 & H_0^{\downarrow\downarrow}(\mathbf{k}) \end{bmatrix} + \begin{bmatrix} H_{SO}^{\uparrow\uparrow} & H_{SO}^{\uparrow\downarrow} \\ H_{SO}^{\downarrow\uparrow} & H_{SO}^{\downarrow\downarrow} \end{bmatrix}. \quad (1)$$

The Hamiltonian without the spin-orbit terms (i.e., $H_0^{\alpha\alpha}(\mathbf{k})$, $\alpha = \uparrow$ or \downarrow) has been given in Ref. 14, the tight-binding parameters are listed in Table I of Ref. 14, and the renormalized spin-orbit splittings of the anion and cation p states (e.g., $\Delta_N = 9$ meV and $\Delta_{Al} = 24$ meV) in $H_{SO}(\mathbf{k})$ have been reported in Refs. 10 and 11. In this letter, only the results for AlN will be shown as an example for studying the Dresselhaus effect.

^{a)}Electronic mail: chiang@mail.phys.nsysu.edu.tw

^{b)}Electronic mail: melee@nknuc.nknu.edu.tw

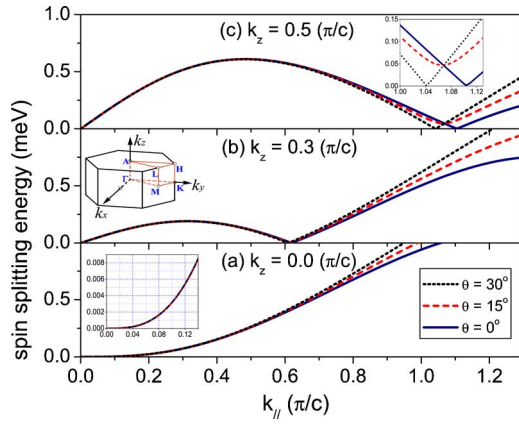


FIG. 1. (Color online) Spin-splitting energy as a function of k_{\parallel} for $\theta = 0^\circ$, 15° , and 30° on the planes of (a) $k_z = 0$, (b) $k_z = 0.3\pi/c$, and (c) $k_z = 0.5\pi/c$ using the LCAO method. The first Brillouin zone with symmetry points is shown in the inset of (b).

Figure 1 shows the absolute values of the spin-splitting energy (i.e., $|\delta E(k_{\parallel}, \theta, k_z)|$) as a function of k_{\parallel} for $\theta = 0^\circ$, 15° , and 30° in the planes of (a) $k_z = 0$, (b) $k_z = 0.3\pi/c$, and (c) $k_z = 0.5\pi/c$. It is seen that in each k_z plane, the three curves ($\theta = 0^\circ$, 15° , and 30°) are strongly θ dependent for $k_{\parallel} > 0.9\pi/c$. However, as k_{\parallel} decreases, they become less θ dependent. They even become nearly θ independent when $k_{\parallel} < 0.6\pi/c$. These imply that the LCAO Hamiltonian exhibits a sixfold symmetry at large k_{\parallel} but exhibits a circular-symmetry-like behavior at small k_{\parallel} . We refer to this phenomenon as the wurtzite rotation symmetry (WRS) effect. The most interesting phenomenon found in Fig. 1 is that each curve exhibits a MSS point located at $k_{\parallel}^{\text{MSS}}(k_z, \theta)$ [note that $k_{\parallel}^{\text{MSS}}(0, \theta) = 0$]. This means that a cone-shaped MSS surface exists in the ideal wurtzite Brillouin zone. The MSS surface can be regarded as a spin-degenerate surface because the spin splitting on the MSS surface is generally very weak. For the spin degeneracy, specifically speaking, there are 12 spin-degenerate lines on the MSS surface and they appear only when θ equals 0° and integer multiples of 30° [see inset of Fig. 1(c)]. Totally, there are 13 spin-degenerate lines in the Brillouin zone if the spin-degenerate line $\bar{\Gamma}A$ ($k_{\parallel} = 0$) due to time-reversal symmetry is also included.

Figure 2 shows the projections of the MSS surface (solid lines) and the spin-degenerate surface of $k_{\parallel}^2 - 4.028k_z^2 = 0 = \delta E$ (dash lines) onto the planes of (i) $k_z = 0.2\pi/c$, (ii) $k_z = 0.4\pi/c$, and (iii) $k_z = 0.6\pi/c$. It is seen that the projections of the spin-degenerate surface (dashed lines) exhibit a circular-symmetry behavior, while the projections of the MSS surface (solid lines) exhibit a wurtzite-rotation-symmetry behavior. It is also seen that the dash line and solid line are nearly identical at small k_z [see Fig. 2(i)] but have significant difference at large k_z [see Fig. 2(iii)]. These indicate that the hexagonal-cone-shaped MSS surface can be well described by a circular-cone-shaped spin-degenerate surface (i.e., $bk_z^2 - k_{\parallel}^2 = 0 = \delta E$, $b = 4.028$) when k_z is not too large due to the WRS effect. The existence of the spin-degenerate surface $bk_z^2 - k_{\parallel}^2 = 0$ implies that the spin-splitting energy δE near the $\bar{\Gamma}$ point can be written in the form of $\delta E = 2\gamma_{wz}k_{\parallel}(bk_z^2 - k_{\parallel}^2)$, in which $\delta E = k_{\parallel} = 0$ represents the spin-degenerate line $\bar{\Gamma}A$. When the spin directions are also taken into account^{7,18} the spin-orbit component of the two-band $\mathbf{k} \cdot \mathbf{p}$ Hamiltonian $H_{\text{SO}}(\mathbf{k})$ can be written as

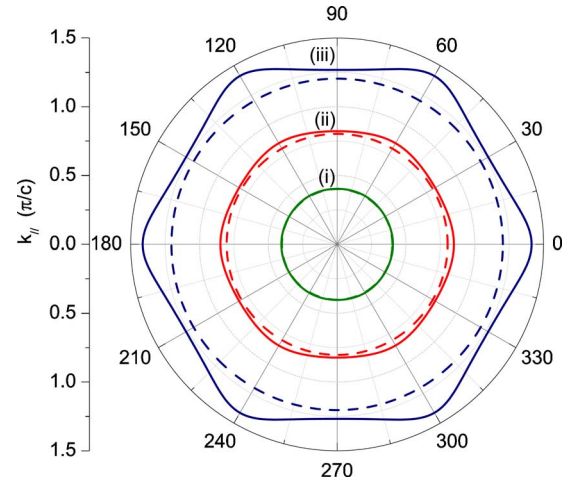


FIG. 2. (Color online) Projections of the minimum spin-splitting surface (solid lines) and the reference spin-degenerate surface $k_{\parallel}^2 = 4.028k_z^2$ (dash lines) onto the planes of (i) $k_z = 0.2\pi/c$, (ii) $k_z = 0.4\pi/c$, and (iii) $k_z = 0.6\pi/c$.

$$H_{\text{SO}}(\mathbf{k}) = \gamma_{wz}(bk_z^2 - k_{\parallel}^2)(\sigma_x k_y - \sigma_y k_x). \quad (2)$$

Here the spin directions are determined by examining the conduction-band eigenvectors of the LCAO Hamiltonian. The value of γ_{wz} evaluated from the k_{\parallel}^3 -dependent curve in the inset of Fig. 1(a) is about 0.74 meV \AA^3 . This confirms that in the nearest-neighbor LCAO model, ideal wurtzite structure yields the cubic- k terms of $\gamma_{wz}(bk_z^2 - k_{\parallel}^2)(\sigma_x k_y - \sigma_y k_x)$ in the two-band $\mathbf{k} \cdot \mathbf{p}$ Hamiltonian. This phenomenon is referred to as the Dresselhaus effect in bulk wurtzite. Note that in the above equation [Eq. (2)], the high-order terms have been neglected. When the high-order terms are also taken into account, the spin-degenerate surface will become a MSS surface. The coefficients b for some other ideal wurtzite materials (b^β , $\beta = \text{ZnO, CdS, CdSe, and ZnS}$) were also calculated. It is interesting to find that \sqrt{b} is nearly equal to the ratio of the average length of $\bar{\Gamma}M$ and $\bar{\Gamma}K$ to $\bar{\Gamma}A$ [see inset of Fig. 1(b)] for all the wurtzite materials (i.e., $\sqrt{b} \approx (\bar{\Gamma}M + \bar{\Gamma}K)/(2\bar{\Gamma}A) = 2.032$). This means that the Dresselhaus effect mentioned above is valid for all the wurtzite materials.

From the above discussions, we conclude that the Dresselhaus effect yields the cubic- k terms shown in Eq. (2), and therefore, produces a cone-shaped MSS surface in the Brillouin zone. When the WSIA effect is also taken into account in Eq. (2), the two-band $\mathbf{k} \cdot \mathbf{p}$ Hamiltonian becomes $H_{\text{SO}}(\mathbf{k}) = [\alpha_{wz} - \gamma_{wz}(k_{\parallel}^2 - bk_z^2)](\sigma_x k_y - \sigma_y k_x)$, where α_{wz} is the WSIA coefficient. This explains why the WSIA effect (s - p_z mixing at $k = 0$) can change the shape of the MSS surface. As shown in Fig. 3, the MSS surface for real wurtzite AlN has a shape of hexagonal hyperboloid of two sheets [Fig. 3(b)], but the MSS surface for ideal wurtzite AlN has a shape of hexagonal cone [Fig. 3(a)]. Here the band structures for real wurtzite AlN are obtained by differentiating the bond in the [001] direction from three other bonds.¹⁹ Certainly, the MSS surface will have a shape of hexagonal hyperboloid of one sheet if $\alpha_{wz}/\gamma_{wz} > 0$ [Please refer to Fig. 1(a) of Ref. 16.]. If the WSIA effect (e.g., strain induced WSIA effect) is extremely strong, the MSS surface may be completely eliminated. The strong coupling between the conduction bands (e.g., $\Delta_{C1} - \Delta_{C3}$ coupling¹² in GaN) should also have significant influence on the shape of the MSS surface. Its influence

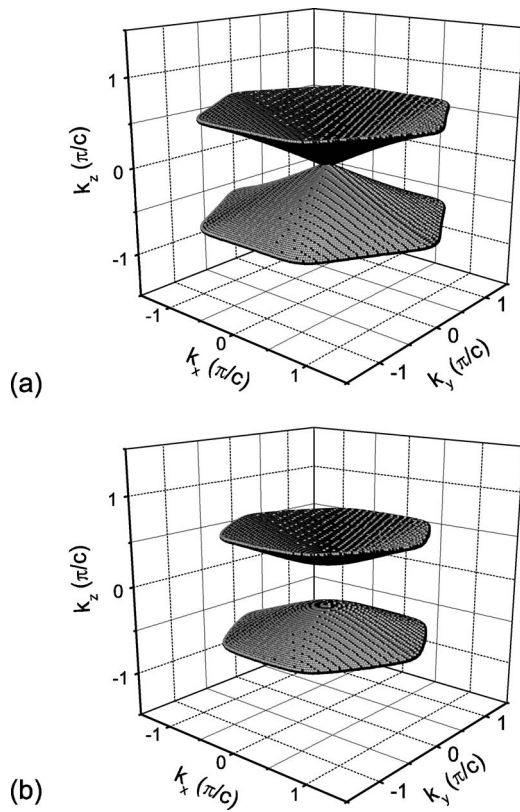


FIG. 3. Three-dimensional plot of the minimum spin-splitting surface for (a) ideal wurtzite and (b) real wurtzite in k space for various k_z 's.

is currently under investigation using the second-nearest-neighbor LCAO method and will be reported in the near future. The spin splitting energies for real wurtzite AlN were also calculated using the local-density approximation (LDA) of the density-functional theory (DFT). The DFT-LDA results confirm the fact that the MSS surface for real wurtzite AlN has a shape of hexagonal hyperboloid of two sheets.

In the two-band $\mathbf{k} \cdot \mathbf{p}$ model, the 2D wurtzite Hamiltonian can be written as^{7,18}

$$H_{IA}(\mathbf{k}) = [\alpha_{IA} - \gamma_{wz} k_{\parallel}^2](\sigma_x k_y - \sigma_y k_x), \quad (3)$$

and the effective spin splitting becomes $\delta E(k) = 2[\alpha_{IA} k_{\parallel} - \gamma_{wz} k_{\parallel}^3]$. Here $\alpha_{IA} = \alpha_R + \alpha_{BIA}$, $\alpha_{BIA} = \alpha_{wz} + \gamma_{wz} b(k_z^2)$, and α_R is the Rashba coefficient. Clearly, a spin-degenerate Fermi surface given by $\alpha_R + \alpha_{BIA} - \gamma_{wz} k_F^2 = 0$ can be achieved in 2DEGs of wurtzite heterostructures by varying k_{\parallel} (e.g., carrier concentration), α_R (e.g., gate voltage), α_{wz} (e.g., crystal field or strain), and $b(k_z^2)$ (e.g., quantum well width). These phenomena indeed have been partly observed in the experiments.^{15,16} The 2D [001]-grown wurtzite Hamiltonian is indeed very similar to the 2D [111]-grown zinc-blende Hamiltonian, except that the former does not have the σ_z component of the k^3 terms [i.e., $\gamma(3k_x^2 - k_y^2)k_y \sigma_z / \sqrt{6}$ as shown in Eq. (9) of Ref. 4, where z is oriented along the growth direction]. The Dresselhaus effect yields a σ_z component of the k^3 terms in 2D [111] zinc-blende Hamiltonian but not in 2D [001] wurtzite Hamiltonian because the wurtzite crystals have a sixfold rotation [001]-axis symmetry but the zinc-blende crystals have a threefold rotation [111]-axis symmetry. Thus, we suggest that the [001] wurtzite QWs (e.g., GaN/AlN) are also the potential candidates for spintronic devices such as the RSL transistor,^{2,3} in addition to the [111]

zinc-blende QWs.^{4,5} Note that, due to our calculations, the three spin lifetime components all show a resonant behavior in [001] wurtzite QWs, when the Fermi surface is spin degenerate.⁵ This reveals the importance of the Dresselhaus effect, because it generates a spin-degenerate surface near the Γ point in the wurtzite Brillouin zone. The spin-degenerate Fermi surface, which has been observed in the n -type GaN QWs,¹⁶ is also expected to be observed experimentally in the p -type GaAs QWs.²⁰

In conclusion, the Dresselhaus effect in ideal bulk wurtzite has been investigated using the nearest-neighbor scheme of the LCAO method. It is demonstrated that the Dresselhaus effect yields a hexagonal-cone-shaped MSS surface in the ideal wurtzite Brillouin zone. The hexagonal-cone-shaped MSS surface can be regarded as circular-cone-shaped spin-degenerate surface in the vicinity of the Γ point. This indicates that the k^3 terms generated by the Dresselhaus effect can be written as $\gamma_{wz}(bk_z^2 - k_{\parallel}^2)(\sigma_x k_y - \sigma_y k_x)$ ($b \approx 4$) in the two-band $\mathbf{k} \cdot \mathbf{p}$ Hamiltonian. The Dresselhaus effect yields a spin-degenerate surface in bulk wurtzite but not in bulk zinc blende, simply because the wurtzite crystals (sixfold rotation [001] axis) have a higher rotation symmetry than the zinc-blende crystals (threefold rotation [111] axis). The existence of the spin-degenerate surface makes the [001]-wurtzite QW (e.g., GaN/AlN) a potential candidate for spintronic devices such as the RSL transistor.

This project was supported by the National Research Council of Taiwan and Academia Sinica.

¹S. Datta and B. Das, Appl. Phys. Lett. **56**, 665 (1990).

²J. Schliemann, J. C. Egues, and D. Loss, Phys. Rev. Lett. **90**, 146801 (2003).

³X. Cartoixa, D. Z.-Y. Ting, and Y.-C. Chang, Appl. Phys. Lett. **83**, 1462 (2003).

⁴X. Cartoixa, D. Z.-Y. Ting, and Y.-C. Chang, Phys. Rev. B **71**, 45313 (2005).

⁵W. T. Wang, Y.-C. Chang, Ikai Lo, and Jih-Chen Chiang (unpublished).

⁶G. Dresselhaus, Phys. Rev. **100**, 580 (1955); E. I. Rashba and V. I. Sheka, Sov. Phys. Solid State **3**, 1257 (1961).

⁷R. I. Rashba, Sov. Phys. Solid State **2**, 1109 (1960); Yu. A. Bychkov and E. I. Rashba, J. Phys. C **17**, 6039 (1984).

⁸E. O. Kane, in *Semiconductors and Semimetals*, edited by R. K. Willardson and A. C. Beer (Academic, New York, 1966), Vol. 1, pp. 75–100.

⁹E. A. de Andrada e Silva, G. C. La Rocca, and F. Bassani, Phys. Rev. B **50**, 8523 (1994).

¹⁰D. J. Chadi, Phys. Rev. B **16**, 790 (1977).

¹¹J. C. Phillips, *Bonds and Bands in Semiconductors* (Academic, San Diego, CA, 1973), p. 179.

¹²Ikai Lo, W. T. Wang, M. H. Gau, S. F. Tsay, and J. C. Chiang, Phys. Rev. B **72**, 245329 (2005).

¹³L. C. Lew Yan Voon, M. Willatzen, M. Cardona, and N. E. Christensen, Phys. Rev. B **53**, 10703 (1996), and references therein.

¹⁴A. Kobayashi, O. F. Sankey, S. M. Volz, and J. D. Dow, Phys. Rev. B **28**, 935 (1983).

¹⁵K. Tsubaki, N. Maeda, T. Saitoh, and N. Kobayashi, Appl. Phys. Lett. **80**, 3126 (2002).

¹⁶Ikai Lo, M. H. Gau, J. K. Tsai, Y. L. Chen, Z. J. Chang, W. T. Wang, Jih-Chen Chiang, and T. Aggerstam, Phys. Rev. B **75**, 245307 (2007).

¹⁷Ikai Lo, J. K. Tsai, W. J. Yao, P. C. Ho, L. W. Tu, T. C. Chang, S. Elhamri, W. C. Mitchel, K. Y. Hsieh, J. H. Huang, H. L. Huang, and W. C. Tsai, Phys. Rev. B **65**, 161306R (2002).

¹⁸W. Weber, S. D. Ganichev, S. N. Danilov, D. Weiss, W. Prettl, Z. D. Kvon, V. V. Bel'kov, L. E. Golub, Hyun-Ick Cho, and Jung-Hee Lee, Appl. Phys. Lett. **87**, 262106 (2005).

¹⁹Atsuko Niwa, Tsukuru Ohtoshi, and Takao Kuroda, Appl. Phys. Lett. **70**, 2159 (1997).

²⁰E. I. Rashba and E. Ya. Sherman, Phys. Lett. A **129**, 175 (1988).